Journal of Basic and Applied Pharmacology
Vol. 3 No. 1 January- June 2023

Page: [O29-44]

Original research article

Elucidating the effects of antimycin A on metabolome of pancreatic beta cells using liquid chromatography-mass spectrometry

Surachai Ngamratanapaiboon[1*], Pracha Yambangyang[2], Pilaslak Akrachalanont[3], Patipol Hongthawonsiri[4], Krittaboon Pornchokchai[4], Siriphattarinya Wongpitoonmanachai[4], Petchlada Pholkla[4], Napatarin Srikornvit[4], Jiajun Mo[4], Watcharaporn Devakul Na Ayutthaya[1]

[1]*Division of Pharmacology, Department of Basic Medical Sciences, Faculty of Medicine Vajira Hospital, Navamindradhiraj University, Dusit, Bangkok, 10300, Thailand*
[2]*Department of Biomedical Engineering, Faculty of Engineering, Mahidol University, Salaya, Nakhon Pathom, 73170, Thailand*
[3]*Department of Medical Sciences, Ministry of Public Health, Nonthaburi, 11000, Thailand*
[4]*Medical Student in Doctor of Medicine Programme, Faculty of Medicine Vajira Hospital, Navamindradhiraj University, Dusit, Bangkok, 10300, Thailand*

Received 10 April 2023; Received in revised form 5 June 2023
Accepted 14 June 2023; Available online 23 June 2023

ABSTRACT

Type 2 diabetes mellitus (T2DM) is a chronic metabolic disorder characterized by impaired glucose homeostasis, insulin resistance, and beta cell dysfunction. Emerging evidence suggests that the mitochondrial electron transport chain (ETC) plays a pivotal role in regulating beta cell function and glucose homeostasis. Antimycin A is a known inhibitor of the mitochondrial ETC complex III, which could potentially impact beta cell metabolism and function. In this study, we aimed to investigate the effect of antimycin A on beta cell metabolism using a metabolomics-based LC-MS approach. Murine pancreatic beta cells (MIN 6) were treated with antimycin A (1 µM) for 2 hr. Control cells were treated with glucose. Metabolites were extracted from the cells, and LC-MS analysis was performed using a high-resolution mass spectrometer. Metabolic profiling was performed using the MetaboAnalyst 5.0. Metabolites were identified and quantified using a metabolite library. Statistical analysis was performed using multivariate and univariate approaches. Metabolic profiling of antimycin A -treated beta cells revealed significant alterations in cellular metabolism compared to control cells. The most significant changes were observed in the metabolism of amino acid, nucleotides, and the tricarboxylic acid (TCA) cycle. Antimycin A can affect these, possibly leading to insulin secretion impairment. The results of this study highlight the potential of antimycin A as a valuable tool for exploring the impact of mitochondrial function on beta cell metabolism and function. The observed changes in metabolite profiles in antimycin A-treated cells shed light on the metabolic pathways crucial for beta cell function and may offer valuable insights for the development of novel diabetes therapies. The metabolomics analysis conducted using LC-MS

***Corresponding author:** surachai.n@nmu.ac.th

in this study represents a powerful approach for investigating the consequences of mitochondrial dysfunction on cellular metabolism.

Keywords: Antimycin A, MIN6 cells, metabolome, liquid chromatography-mass spectrometry

1. Introduction

Type 2 diabetes mellitus (T2DM) is a long-lasting metabolic condition that is identified by disrupted regulation of glucose levels, decreased sensitivity to insulin, and malfunctioning of beta cells. Recent findings indicate that the mitochondrial electron transport chain (ETC) has a crucial influence on the control of beta cell function and the maintenance of glucose homeostasis. The electron transport chain (ETC) in the mitochondria is an essential component of cellular respiration that generates ATP.[1] Antimycin A is a well-known inhibitor of complex III in the ETC and has been used to investigate the role of the ETC in cellular physiology and pathology.[2,3] However, the precise impact of antimycin A on cellular metabolism remains unclear, especially in beta cell function.

Metabolomics is a powerful tool for studying the effects of various perturbations on cellular metabolism.[4-6] Liquid chromatography-mass spectrometry (LC-MS) is a commonly used technique for metabolomics studies because of its sensitivity, selectivity, and accuracy.[7-9] In recent years, LC-MS-based metabolomics has been increasingly used to study the effects of mitochondrial dysfunction on cellular metabolism.[10-12]

This study aims to use LC-MS-based metabolomics to investigate the effects of antimycin A on the metabolome of murine pancreatic beta cells (MIN6). MIN6 cells are a relevant model system for studying the effects of mitochondrial dysfunction on pancreatic function and the development of pancreatic diseases such as diabetes and pancreatic cancer. To the best of our knowledge, there has been no comprehensive study of the effects of antimycin A on the metabolome of MIN6 cells using LC-MS.

Our hypothesis is that antimycin A treatment will result in significant changes in the metabolome of MIN6 cells, indicating disturbances in key metabolic pathways, including glycolysis, the TCA cycle, and amino acid metabolism. Identifying such changes could provide insight into the mechanisms underlying the cytotoxicity of antimycin A and its potential therapeutic uses in pancreatic diseases.

2. Materials and Methods

2.1 Chemicals

MS grade acetonitrile and methanol were procured from Fisher Chemicals (Apex Chemicals, Bangkok, Thailand). Elga Purelab Genetic (RCI labscan, Bangkok, Thailand) was the source of water. MS grade formic acid was obtained from Acros Organics (DKSH Group, Bangkok, Thailand), and Sigma-Aldrich (Merck, Bangkok, Thailand) was the supplier for all other chemical compounds used. It is noteworthy that all the chemical compounds used in this study were of MS grade quality.

2.2 MIN6 cells

MIN6 cells (a gift from Paul A. Smith, The University of Nottingham, UK) were cultured in RPMI-1640 medium supplemented with 10% fetal bovine serum (FBS), 100 U/ml peFnicillin, and 100 μg/ml streptomycin. Cells were maintained at 37°C in a humidified atmosphere of 5% CO_2.

2.3 Cell experiments

MIN6 cells, a murine pancreatic beta cell line, were cultured as previously described by Cataldo et al.[13] Briefly, MIN6 lines (passage 10–13) were treated with 20 μl of 1 M glucose for 7 minutes to give a 10 mM

final concentration. The concentration and time treatment give a maximal insulin secretion, in line with previous reports of glucose-stimulated insulin secretion in islets and INS-1 832/13 cells.[13] The glucose-treated cells were then exposed to 6 µl of glucose solution as a vehicle control or 1 µM antimycin A for 2 h. Each group had six biological replicates. After treatment, MIN6 cells were transferred to fresh Eppendorf tubes and centrifuged for 2 minutes at 1,000 rpm to stop the reaction. MIN6 cell pellets were extracted with cold methanol (4°C) and the cell suspensions vortexed for 2 hr in a cold room (4°C). The suspensions were centrifuged for 10 minutes at 15,000 rpm at 4°C. The supernatants were transferred to new Eppendorf tubes and kept at −80°C for further analysis.

2.4 Insulin assay

The mouse/rat insulin ELISA kits (Merck, Bangkok, Thailand) were used to quantify the insulin concentration of each condition in accordance with the protocol and the manufacturer's guidelines. The summary statistics are presented as mean values along with the standard error of measurements from at least three independent experiments.

2.5 Metabolome extraction

After treatment, cells were washed twice with ice-cold phosphate-buffered saline (PBS) and quenched with 80% methanol at -80°C for 30 minutes. Cells were then scraped and transferred to microcentrifuge tubes. Samples were centrifuged at 14,000 rpm for 10 minutes, and the supernatant was collected. The supernatant was dried using a SpeedVac concentrator and reconstituted in 100 µl of 50% methanol for LC-MS analysis.

2.6 LC-MS analysis

The Thermo Scientific Accela LC systems and the high-resolution MS Q-ExactiveTM (Thermo Scientific, Bangkok, Thailand) were utilized for liquid chromatography. The extracted compounds were separated using a ZIC-pHILIC column (Merck, Bangkok, Thailand) with a particle size of 3.5 µm and dimensions of 150 x 2.1 mm. A ZIC-pHILIC PEEK guard column (Merck, Bangkok, Thailand) with a particle size of 5 µm and dimensions of 20 x 2.1 mm was also employed. The mobile phases consisted of acetonitrile (A) and 20 mM ammonium carbonate (pH 9.2) at a flow rate of 0.2 ml/min at 40°C (B). A gradient was run to 95% B at t=0 minutes, beginning at 5% B, and completed in 13 minutes. A gradient was also run to 5% B and completed in 15 minutes. Following column washing and equilibration, the run ended after 20 minutes with 5% B. Ion detection data were collected in positive and negative ESI modes between 70 and 1,000 m/z. The pooled quality control (QC) sample, which served to evaluate instrument performance, was composed of a 10 µl aliquot from each study sample and was injected during analysis. The LC and MS conditions were established based on a previous study by Ngamratanapaiboon and Yambangyang.[14]

2.7 Metabolite identification and quantification

Raw LC-MS data were processed using Compound Discovery software (version 3.3.1). Peak detection, retention time alignment, and peak grouping were performed using the cent Wave algorithm. Metabolites were identified by comparing the retention time and accurate mass of the peaks with an in-house library of authentic standards and online databases, including METLIN and the Human Metabolome Database (HMDB). Metabolites were quantified using the integrated peak area of the extracted ion chromatogram (EIC) at a mass accuracy of 5 ppm.

2.8 Statistical analysis

Multivariate statistical analysis was performed using principal component analysis (PCA) and partial least squares-discriminant analysis (PLS-DA) using the MetaboAnalyst 5.0. Univariate statistical analysis was performed using the Student's t-test with Benjamini-Hochberg correction for multiple comparisons using MetaboAnalyst software (version 5.0). Metabolites with a fold change >1.5 and a

false discovery rate (FDR) <0. 05 were considered significant.

2.9 Ethical approval

This study did not involve human or animal subjects and did not require ethical approval.

3. Results

3.1 Insulin secretion

The results of the MTS assay revealed that the viability of MIN6 cells remained unaffected by 10 mM glucose or 1 µM antimycin A (data not shown) . The impact of glucose and the combination of glucose and antimycin A on insulin secretion was analyzed as illustrated in Fig. 1. The insulin concentration increased in the glucose-treated group and the combined glucose and antimycin A-treated group in comparison to the untreated group. Nevertheless, antimycin A decreased the insulin concentration in MIN6 cells in comparison to the glucose- treated group (Fig 1). Full scan base peak chromatograms of a control and treated cells are shown in Supplementary Fig. 1 and 2.

3.2 Antimycin A treatment alters metabolome in MIN6

To investigate the effect of antimycin A on beta cell metabolism, we treated MIN6 cells with antimycin A (1 µM) (+ glucose) for 2 hr and compared the metabolite profiles with glucose-treated cells (as a control).

LC-MS analysis of the metabolome (or metabolites) extracts revealed a total of 260 metabolites, including amino acids, organic acids, nucleotides, and lipids. Multivariate statistical analysis using PCA showed clear separation between the antimycin A (+ glucose) -treated cells and control cells, indicating a significant effect of antimycin A on MIN6 cell metabolism (Fig. 2A).

PLS- DA analysis showed that antimycin A treatment significantly altered the metabolite profiles, with 78 metabolites showing a significant difference in abundance (p<0. 05) (Fig. 2B) . These metabolites included amino acids, such as alanine, aspartic acid, and glutamic acid, which were significantly changed in abundance, as well as several organic acids, such as succinic acid, fumaric acid, and malic acid, which were significantly altered in abundance (Supplementary Table.1).

Using MetaboAnalyst 5.0, the metabolites revealed antimycin A-related pathways which had a probability of less than 0.01 and an impact greater than 0.20, as shown in Fig. 3, including purine (nucleotide) metabolism, amino acid metabolism, and The Citrate cycle (also known as the TCA cycle). These results suggest that antimycin A treatment alters beta cell metabolism by inhibiting the mitochondrial electron transport chain complex III and causing a shift in the metabolic pathways involved in energy production and biosynthesis as indicated in Fig. 4. The altered metabolite profiles may have implications for beta cell function and insulin secretion, highlighting the potential role of mitochondrial function in beta cell health and disease.

3.3 Validation of antimycin A-induced changes in MIN6 cell metabolism

To validate the LC-MS results, we performed targeted metabolomics analysis using a quantitative assay for selected metabolites by investigating retention times and peak areas of the selected metabolites (data not shown). We selected 9 metabolites with significant changes in abundance in the antimycin A-treated cells, including AMP, ADP, ATP, succinic acid, fumaric acid, citric acid/ isocitric acid, L- aspartic acid, L-asparagine, and L-glutamine (Table 1).

Consistent with the LC-MS results, the targeted metabolomics analysis showed a significant increase in the levels of AMP, ADP, and succinic acid in antimycin A + glucose- treated cells compared to glucose-treated cells (Fig.4). In addition, the levels of the others were significantly decreased (Table 1).

4. Discussion

Antimycin A is a potent inhibitor of mitochondrial respiration, particularly at the level of complex III in the electron transport chain. This can have significant impacts on beta cell function, which heavily relies on mitochondrial metabolism for ATP generation.

In the current study, we found that the glycerol 3-phosphate, some nucleotides, few metabolites involved in the citric acid cycle, and some amino acids were significantly changed (Table 1).

Antimycin A inhibits mitochondrial respiration, which can lead to decreased ATP production. As a compensatory mechanism, MIN6 cells may upregulate glycolysis to generate ATP through the cytoplasmic pathways. [15] Increased glycolytic flux can result in elevated glucose uptake and metabolism,[16] leading to increased production of glycerol 3-phosphate as an intermediate in the glycolytic pathway.[17] Glycerol 3-phosphate is crucial in both glycolysis and triglyceride synthesis, and its metabolism is closely linked to the production of electron carriers NADH and FADH2, which feed into the electron transport chain.[18] In the presence of antimycin A, glycerol 3-phosphate metabolism may be impaired, reducing ATP production and potentially harming beta cell function.

Moreover, glycerol 3-phosphate plays a crucial role in lipid metabolism, acting as a precursor for the synthesis of triglycerides and phospholipids.[19] Disruption of mitochondrial respiration by antimycin A can affect lipid metabolism pathways (Supplementary Table 1), potentially altering the availability of glycerol 3-phosphate and other metabolites for lipid biosynthesis. Reduced oxidative phosphorylation and ATP levels may impair the synthesis of complex lipids, leading to changes in glycerol 3-phosphate utilization for lipid synthesis.

Additionally, various nucleotides, including AMP, ADP, ATP, and others, are essential in cellular metabolism, with ATP being a critical energy source for beta cells.[20] In particular, ATP is a critical component in beta cell function, as it is required for the release of insulin in response to glucose.[21-23] Decreased ATP production due to antimycin A inhibition can impair insulin secretion (Fig. 1).

Moreover, the citric acid cycle, also called the Krebs cycle or TCA cycle, is a critical metabolic pathway responsible for producing ATP and other essential metabolites.[24-26] Citric acid, malic acid, succinic acid, and fumaric acid all participate in this process. However, antimycin A can impede this pathway by inhibiting it, which can further decrease ATP production, disrupt amino acid metabolism, and ultimately impact beta cell function.

Finally, amino acids also play a significant part in beta cell function as they are necessary for insulin synthesis and release. Several amino acids, including glutamine, alanine, and arginine, have been shown to trigger an increase in glucose-stimulated insulin secretion (GSIS), suggesting that there are shared pathways between β-cell amino acid and glucose metabolism. Mitochondrial metabolism, in particular, plays a critical role in connecting the recognition of amino acids and glucose to the release of insulin granules via exocytosis.[27-28] Antimycin A inhibition can affect amino acid metabolism, possibly leading to insulin secretion impairment.

In conclusion, the use of antimycin A can have significant impacts on beta cell function, which heavily relies on mitochondrial metabolism for ATP generation. In this study, it was found that the inhibition of mitochondrial respiration by antimycin A affected the metabolism of glycerol 3-phosphate, nucleotides, citric acid cycle metabolites, and amino acids, all of which are critical for beta cell function. The impaired metabolism of glycerol 3-phosphate and decreased ATP production due to the inhibition of nucleotide metabolism and the citric acid cycle could impair insulin secretion. Therefore,

antimycin A as an inhibitor of mitochondrial respiration, can have detrimental effects on beta cell function and ultimately affect insulin homeostasis.

5. Conclusion

This study demonstrates the potential of antimycin A as a tool for investigating the role of mitochondrial function in beta cell metabolism and function. The altered metabolite profiles observed in antimycin A-treated cells provide insights into the metabolic pathways involved in beta cell function and may have implications for the development of new therapies for diabetes. The LC-MS-based metabolomics analysis used in this study provides a powerful tool for investigating the effects of mitochondrial dysfunction on cellular metabolism.

Table 1. Metabolites with significant changes in abundance in MIN6 cells treated with antimycin A + glucose compared with glucose treated MIN6 cells.

Metabolite	Anova (p)	Fold Change*
Antimycin A	2.41E-07	0.00
Glycerol 3-phosphate	2.66E-05	0.19
Guanosine monophosphate	4.84E-14	0.20
2'-Deoxyguanosine 5'-diphosphate	1.35E-05	0.22
Adenosine diphosphate	1.24E-05	0.28
Adenosine monophosphate	5.24E-13	0.32
Succinic acid	6.19E-10	0.40
Adenine	6.09E-04	0.46
Adenosine	6.18E-06	0.51
Inosine monophosphate	6.84E-05	0.53
Hypoxanthine	1.47E-05	0.59
Glyceraldehyde	8.76E-04	0.63
Uridine 5'-monophosphate	7.74E-04	0.63
Creatine	7.71E-05	1.50
L-Carnitine	4.01E-05	1.55
L-Glutamine	8.43E-08	1.65
Citric acid/Isocitric acid	4.20E-04	2.19
L-Asparagine	1.05E-07	2.27
N-Acetyl-D-Glucosamine 6-Phosphate	3.27E-06	2.30
Adenosine triphosphate	3.54E-13	2.52
Uracil	3.27E-06	3.60

*Fold change = Level of metabolite in glucose-treated MIN6 cells/ Level of metabolite in antimycin A + glucose-treated MIN6 cells.

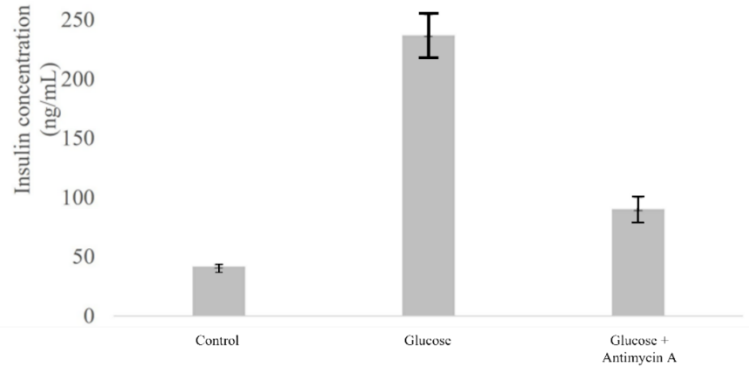

Fig. 1. Graphic presentation of the insulin concentration of the MIN6 cells untreated or subjected to glucose treatment or combined glucose and antimycin A treatment, respectively.

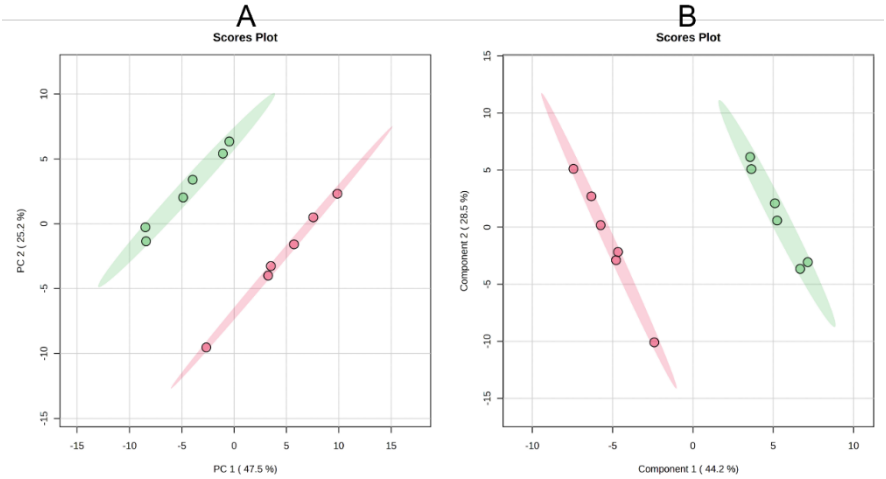

Fig. 2. Multivariate statistical analysis of metabolite profiles in MIN6 cells treated with antimycin A. (A) PCA score plot showing clear separation between glucose treatment (green), and antimycin A + glucose treatment (pink). (B) PLS-DA score plot showing significant differences in metabolite profiles among control (green), glucose treatment (violet), and antimycin A + glucose treatment.

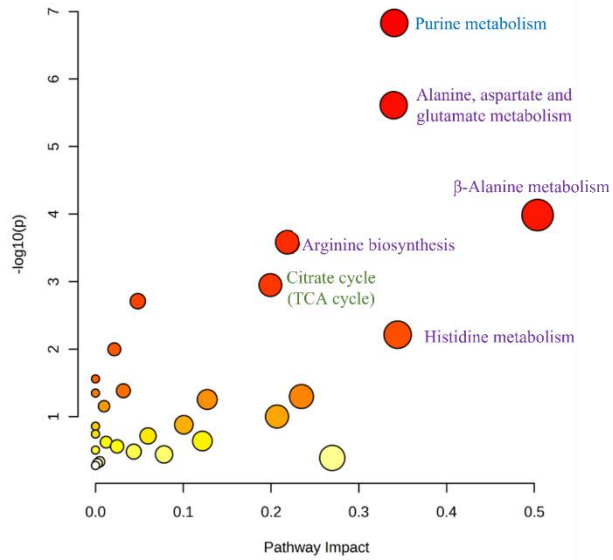

Fig. 3. The identification of pathways involving X metabolites that distinguished between glucose and glucose + antimycin A treatments. To generate the plot, MetaboAnalyst 5.0 was utilized, with the x-axis depicting the impact of the discovered metabolites on the indicated pathway, while the y-axis illustrates the relatively abundant metabolites in the designated pathway. The significance of pathway enrichment is indicated by the color of the circles, with the size of the circle representing the pathway's impact.

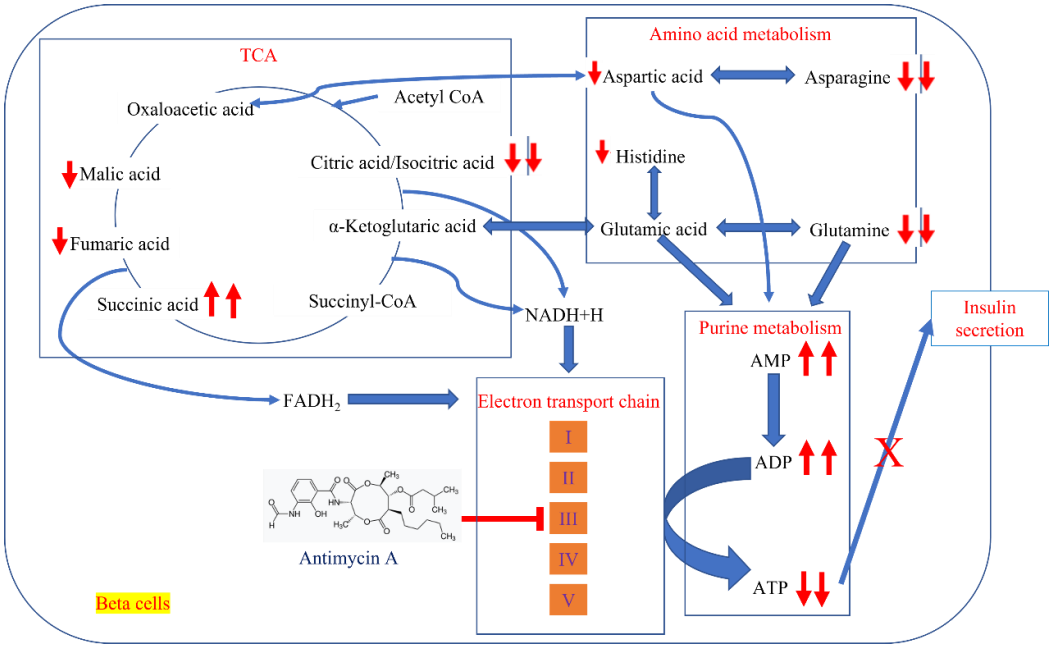

Fig. 4. Possible metabolic pathways related to antimycin A effects on beta cell metabolism. The metabolic pathways that exhibited the most notable alterations were those related to amino acid metabolism, nucleotide metabolism, and the tricarboxylic acid (TCA) cycle. The red arrows indicate the direction of change.

Acknowledgements

We would like to thank Paul A. Smith (School of Life Sciences, University of Nottingham Medical School, Queens Medical Centre, Nottinghamshire, NG7 2UH, UK) for providing us with MIN6 cells.

Conflicts of Interest

The authors declared no conflict of interest in this study.

References

[1] Nolfi-Donegan D, Braganza A, Shiva S. Mitochondrial electron transport chain: Oxidative phosphorylation, oxidant production, and methods of measurement. Redox Biol. 2020;37:101674.

[2] Hytti M, Korhonen E, Hyttinen JMT, Roehrich H, Kaarniranta K, Ferrington DA, Kauppinen A. Antimycin A-induced mitochondrial damage causes human RPE cell death despite activation of autophagy. Oxid Med Cell Longev. 2019;2019:1583656.

[3] Ma X, Jin M, Cai Y, Xia H, Long K, Liu J, et al. Mitochondrial electron transport chain complex III is required for antimycin A to inhibit autophagy. Chem Biol. 2011;18(11): 1474-1481.

[4] Bauermeister A, Mannochio-Russo H, Costa-Lotufo LV, Jarmusch AK, Dorrestein PC. Mass spectrometry-based metabolomics in microbiome investigations. Nat Rev Microbiol. 2022;20(3):143-160.

[5] Muthubharathi BC, Gowripriya T, Balamurugan K. Metabolomics: small molecules that matter more. Mol Omics. 2021;17(2):210-229.

[6] Rinschen MM, Ivanisevic J, Giera M, Siuzdak G. Identification of bioactive metabolites using activity metabolomics. Nat Rev Mol Cell Biol. 2019;20(6):353-367.

[7] Reveglia P, Paolillo C, Ferretti G, Carlo AD, Angiolillo A, Nasso R, et al. Challenges in LC-MS-based metabolomics for Alzheimer's disease early detection: targeted approaches versus untargeted approaches. Metabolomics. 2021;17(9):78.

[8] Dator R, Villalta PW, Thomson N, Jensen J, Hatsukami DK, Stepanov I, et al. Metabolomics profiles of smokers from two ethnic groups with differing lung cancer risk. Chem Res Toxicol. 2020;33(8): 2087-2098.

[9] Muelas MW, Roberts I, Mughal F, O'Hagan S, Day PJ, Kell DB. An untargeted metabolomics strategy to measure differences in metabolite uptake and excretion by mammalian cell lines. Metabolomics. 2020;16(10):107.

[10] Danzi F, Pacchiana R, Mafficini A, Scupoli MT, Scarpa A, Donadelli M, et al. To metabolomics and beyond: a technological portfolio to investigate cancer metabolism. Sig Transduct Target Ther. 2023;8(137):1-22.

[11] Alarcon-Barrera JC, Kostidis S, Ondo-Mendez A, Giera M. Recent advances in metabolomics analysis for early drug development. Drug Discov Today. 2022; 27(6):1763-1773.

[12] van der Walt G, Lindeque JZ, Mason S, Louw R. Sub-cellular metabolomics contributes mitochondria-specific metabolic insights to a mouse model of Leigh syndrome. Metabolites. 2021;11(10):658.

[13] Cataldo LR, Cortés VA, Mizgier ML, Aranda E, Mezzano D, Olmos P, et al. Fluoxetine impairs insulin secretion without modifying extracellular serotonin levels in MIN6 β-cells. Exp Clin Endocrinol Diabetes. 2015;123(8):473-478.

[14] Ngamratanapaiboon S, Yambangyang P. Quantification of antipsychotic biotransformation in brain microvascular endothelial cells by using untargeted metabolomics. Drug Discov Ther. 2021;15(6):317-324.

[15] Pizarro-Delgado J, Deeney JT, Corkey BE, Tamarit-Rodriguez J. Direct stimulation of islet insulin secretion by glycolytic and mitochondrial metabolites in KCl-depolarized islets. PLoS One.2016;11(11):e0166111.

[16] Marek CB, Peralta RM, Itinose AM, Bracht A. Influence of tamoxifen on gluconeogenesis and glycolysis in the perfused rat liver. Chem Biol Interact. 2011;193(1):22-33.

[17] Al-Mass A, Poursharifi P, Peyot ML, Lussier R, Levens EJ, Guida J, et al. Glycerol-3-phosphate phosphatase operates a glycerol shunt in pancreatic β-cells that controls insulin secretion and metabolic stress. Mol Metab. 2022;60:101471.

[18] Possik E, Al-Mass A, Peyot ML, Ahmad R, Al-Mulla F, Madiraju SRM, et al. New mammalian glycerol-3-phosphate phosphatase: role in β-Cell, liver and adipocyte metabolism.

Front Endocrinol (Lausanne). 2021;12:706607.
[19] Swierczynski J, Zabrocka L, Goyke E, Raczynska S, Adamonis W, Sledzinski Z. Enhanced glycerol 3-phosphate dehydrogenase activity in adipose tissue of obese humans. Mol Cell Biochem. 2003;254(1-2):55-59.
[20] Bonora M, Patergnani S, Rimessi A, Marchi ED, Suski JM, Bononi A, et al. ATP synthesis and storage. Purinergic Signal. 2012;8(3):343-357.
[21] Fridlyand LE, Jacobson DA, Philipson LH. Ion channels and regulation of insulin secretion in human β-cells: a computational systems analysis. Islets. 2013;5(1):1-15.
[22] Duvoor C, Dendi VS, Marco A, Shekhawat NS, Chada A, Ravilla R, Musham CK, et al. Commentary: ATP: The crucial component of secretory vesicles: accelerated ATP/insulin exocytosis and prediabetes. Front Physiol. 2017;8:53.
[23] Li J, Yan H, Xiang R, Yang W, Ye J, Yin R, et al. ATP secretion and metabolism in regulating pancreatic beta cell functions and hepatic glycolipid metabolism. Front Physiol. 2022;13:918042.
[24] Judge A, Dodd MS. Metabolism. Essays Biochem. 2020;64(4):607-647.
[25] Martínez-Reyes I, Chandel NS. Mitochondrial TCA cycle metabolites control physiology and disease. Nat Commun. 2020;11(1):102.
[26] Chakrabarty RP, Chandel NS. Mitochondria as signaling organelles control mammalian stem cell fate. Cell Stem Cell. 2021;28(3):394-408.
[27] Newsholme P, Krause M. Nutritional regulation of insulin secretion: implications for diabetes. Clin Biochem Rev. 2012;33(2):35-47.
[28] Fu Z, Gilbert ER, Liu D. Regulation of insulin synthesis and secretion and pancreatic Beta-cell dysfunction in diabetes. Curr Diabetes Rev. 2013;9(1):25-53.

Supplementary Table 1

Detected m/z	Retention time (min)	Metabolite	Formula	Monoisotopic mass	Adduct	Calculated m/z	Delta (ppm)	Anova (p)	Fold Change (Conrol/ Actinomycin)
87.0089	8.62	Malonic semialdehyde	$C_3H_4O_3$	88.0160	$[M-H]^-$	87.0088	1	2.16E-03	1.13
87.0089	2.54	Pyruvic acid	$C_3H_4O_3$	88.0160	$[M-H]^-$	87.0088	1	5.74E-05	1.09
90.0551	8.87	beta-Alanine	$C_3H_7NO_2$	89.0477	$[M+H]^+$	90.0550	1	1.98E-07	0.93
89.0246	2.63	Glyceraldehyde	$C_3H_6O_3$	90.0317	$[M-H]^-$	89.0244	2	8.76E-04	0.63
101.0245	8.60	2-Ketobutyric acid	$C_4H_6O_3$	102.0317	$[M-H]^-$	101.0244	1	1.75E-14	1.03
112.0507	7.61	Cytosine	$C_4H_5N_3O$	111.0433	$[M+H]^+$	112.0505	1	1.21E-04	0.78
110.9854	8.11	Methylphosphate	CH_5O_4P	111.9925	$[M-H]^-$	110.9853	1	6.30E-07	1.71
111.0201	6.37	Uracil	$C_4H_4N_2O_2$	112.0273	$[M-H]^-$	111.0200	1	4.38E-04	3.60
115.0038	8.87	Fumaric acid	$C_4H_4O_4$	116.0110	$[M-H]^-$	115.0037	1	6.45E-13	1.37
117.0195	8.24	Succinic acid	$C_4H_6O_4$	118.0266	$[M-H]^-$	117.0193	1	6.19E-10	0.40
125.0012	7.47	Dimethylphosphate	$C_2H_7O_4P$	126.0082	$[M-H]^-$	125.0009	2	2.54E-04	1.27
130.0864	7.94	D-Pipecolic acid	$C_6H_{11}NO_2$	129.0790	$[M+H]^+$	130.0863	1	9.54E-05	1.39
132.0769	8.87	Creatine	$C_4H_9N_3O_2$	131.0695	$[M+H]^+$	132.0768	1	3.26E-05	1.50
133.0610	9.10	L-Asparagine	$C_4H_8N_2O_3$	132.0535	$[M+H]^+$	133.0608	2	1.05E-07	2.27
133.0860	2.60	Leucinic acid	$C_6H_{12}O_3$	132.0786	$[M+H]^+$	133.0859	1	6.52E-05	0.91
132.0304	8.75	L-Aspartic acid	$C_4H_7NO_4$	133.0375	$[M-H]^-$	132.0302	1	3.51E-05	1.12
133.0144	8.82	Malic acid	$C_4H_6O_5$	134.0215	$[M-H]^-$	133.0142	1	1.02E-09	1.29
134.0474	6.13	Adenine	$C_5H_5N_5$	135.0545	$[M-H]^-$	134.0472	1	1.75E-05	0.46
137.0459	6.58	2-Hydroxypurine	$C_5H_4N_4O$	136.0385	$[M+H]^+$	137.0458	1	8.77E-06	0.66
137.0459	7.29	Hypoxanthine	$C_5H_4N_4O$	136.0385	$[M+H]^+$	137.0458	1	1.47E-05	0.59
139.0503	2.60	Urocanic acid	$C_6H_6N_2O_2$	138.0429	$[M+H]^+$	139.0502	1	1.13E-05	0.68

Detected m/z	Retention time (min)	Metabolite	Formula	Monoisotopic mass	Adduct	Calculated m/z	Delta (ppm)	Anova (p)	Fold Change (Conrol/ Actinomycin)
143.0351	8.65	3-Methylglutaconic acid	$C_6H_8O_4$	144.0423	$[M-H]^-$	143.0350	1	2.11E-08	1.05
146.1177	2.41	4-Trimethylammoniobutanoic acid	$C_7H_{15}NO_2$	145.1103	$[M+H]^+$	146.1176	1	1.22E-03	1.25
147.0765	9.05	L-Glutamine	$C_5H_{10}N_2O_3$	146.0691	$[M+H]^+$	147.0764	1	8.43E-08	1.65
150.1127	5.46	Triethanolamine	$C_6H_{15}NO_3$	149.1052	$[M+H]^+$	150.1125	1	1.08E-10	0.10
152.0566	7.75	Guanine	$C_5H_5N_5O$	151.0494	$[M+H]^+$	152.0567	0	7.08E-05	0.73
156.0769	9.45	L-Histidine	$C_6H_9N_3O_2$	155.0695	$[M+H]^+$	156.0768	1	5.68E-04	1.33
155.0100	6.32	Orotic acid	$C_5H_4N_2O_4$	156.0171	$[M-H]^-$	155.0098	1	3.19E-04	2.06
155.1079	1.92	Fatty acid	$C_9H_{16}O_2$	156.1150	$[M-H]^-$	155.1078	1	4.44E-04	2.56
162.1126	8.52	L-Carnitine	$C_7H_{15}NO_3$	161.1052	$[M+H]^+$	162.1125	1	4.01E-05	1.55
171.0066	8.67	Glycerol 3-phosphate	$C_3H_9O_6P$	172.0137	$[M-H]^-$	171.0064	1	2.66E-05	0.19
176.1031	9.45	Citrulline	$C_6H_{13}N_3O_3$	175.0957	$[M+H]^+$	176.1030	1	4.64E-05	0.84
179.0564	8.62	D-Glucose	$C_6H_{12}O_6$	180.0634	$[M-H]^-$	179.0561	1	2.22E-16	1.07
191.0200	9.84	Citric acid/Isocitric acid	$C_6H_8O_7$	192.0270	$[M-H]^-$	191.0197	1	2.32E-05	2.19
193.0906	1.77	1-Octanesulfonic acid	$C_8H_{18}O_3S$	194.0977	$[M-H]^-$	193.0904	1	1.16E-05	0.02
198.1491	2.50	Estreptoquinasa	$C_{11}H_{19}NO_2$	197.1416	$[M+H]^+$	198.1489	1	3.22E-04	1.30
202.1804	3.87	Caproylcholine	$C_{11}H_{24}NO_2$	202.1807	$[M+H]^+$	202.1807	2	1.74E-09	0.61
204.1232	7.58	L-Acetylcarnitine	$C_9H_{17}NO_4$	203.1158	$[M+H]^+$	204.1230	1	1.83E-08	1.19
216.1960	2.47	Heptanoylcholine	$C_{12}H_{26}NO_2$	216.1964	$[M+H]^+$	216.1964	2	4.00E-04	1.34
232.1546	6.65	Isobutyrylcarnitine/Butyrylcarnitine	$C_{11}H_{21}NO_4$	231.1471	$[M+H]^+$	232.1543	1	4.66E-09	1.24
244.0933	7.61	Cytidine	$C_9H_{13}N_3O_5$	243.0855	$[M+H]^+$	244.0928	2	3.36E-05	0.96
244.1909	2.16	N-Undecanoylglycine	$C_{13}H_{25}NO_3$	243.1834	$[M+H]^+$	244.1907	1	1.68E-05	1.63
246.1702	6.48	Isovalerylcarnitine/Valerylcarnitine	$C_{12}H_{23}NO_4$	245.1627	$[M+H]^+$	246.1700	1	1.36E-06	0.87

Detected m/z	Retention time (min)	Metabolite	Formula	Monoisotopic mass	Adduct	Calculated m/z	Delta (ppm)	Anova (p)	Fold Change (Conrol/ Actinomycin)
260.1858	2.60	Hexanoylcarnitine	$C_{13}H_{25}NO_4$	259.1784	$[M+H]^+$	260.1856	1	3.61E-05	2.92
260.1859	6.16	Hexanoylcarnitine	$C_{13}H_{25}NO_4$	259.1784	$[M+H]^+$	260.1856	1	7.86E-07	2.73
268.1043	6.24	Adenosine	$C_{10}H_{13}N_5O_4$	267.0968	$[M+H]^+$	268.1040	1	6.18E-06	0.51
288.2171	2.60	Octanoylcarnitine/Valproylcarnitine	$C_{15}H_{29}NO_4$	287.2097	$[M+H]^+$	288.2169	1	2.27E-06	1.25
288.2535	2.30	Lauroyl diethanolamide	$C_{16}H_{33}NO_3$	287.2460	$[M+H]^+$	288.2533	0	1.76E-05	1.70
291.2168	2.21	Glycerol 1-(5-hydroxydodecanoate)	$C_{15}H_{30}O_5$	290.2093	$[M+H]^+$	291.2166	1	5.16E-07	0.73
289.2124	2.27	Succinylcholine	$C_{14}H_{30}N_2O_4$	290.2206	$[M+H]^+$	289.2133	3	1.29E-08	0.05
295.0940	1.94	Tyrosyl-Aspartate/Aspartyl-Tyrosine	$C_{13}H_{16}N_2O_6$	296.1008	$[M-H]^-$	295.0936	2	0.00E+00	0.00
297.1084	2.04	Tyrosyl-Aspartate/Aspartyl-Tyrosine	$C_{13}H_{16}N_2O_6$	296.1008	$[M+H]^+$	297.1081	1	0.00E+00	0.00
295.0940	1.95	DHAP(8:0)	$C_{11}H_{21}O_7P$	296.1025	$[M-H]^-$	295.0952	4	0.00E+00	0.00
300.0495	8.70	N-Acetyl-D-Glucosamine 6-Phosphate	$C_8H_{16}NO_9P$	301.0563	$[M-H]^-$	300.0490	2	3.27E-06	2.30
307.1594	1.67	n-Octyl-beta-D-thioglucopyranoside	$C_{14}H_{28}O_5S$	308.1657	$[M-H]^-$	307.1585	3	1.64E-06	0.25
314.2092	2.06	Val-Val-Val	$C_{15}H_{29}N_3O_4$	315.2158	$[M-H]^-$	314.2085	2	2.46E-06	0.35
323.0292	8.67	Uridine 5'-monophosphate	$C_9H_{13}N_2O_9P$	324.0359	$[M-H]^-$	323.0286	2	7.74E-04	0.63
341.1095	9.30	Trehalose	$C_{12}H_{22}O_{11}$	342.1162	$[M-H]^-$	341.1089	2	6.54E-06	0.69
344.2430	1.95	N-Myristoyl Aspartic acid	$C_{18}H_{33}NO_5$	343.2359	$[M+H]^+$	344.2431	1	6.18E-05	1.35
346.2230	2.01	Sebacoyl-L-carnitine	$C_{17}H_{31}NO_6$	345.2151	$[M+H]^+$	346.2224	2	3.42E-05	2.33
346.0564	8.22	Adenosine monophosphate	$C_{10}H_{14}N_5O_7P$	347.0631	$[M-H]^-$	346.0558	2	5.24E-13	0.32
348.0706	8.04	Adenosine triphosphate	$C_{10}H_{14}N_5O_7P$	347.0631	$[M+H]^+$	348.0704	1	3.54E-13	2.52
347.0405	8.87	Inosine monophosphate	$C_{10}H_{13}N_4O_8P$	348.0471	$[M-H]^-$	347.0398	2	6.84E-05	0.53
364.0655	9.42	Guanosine monophosphate	$C_{10}H_{14}N_5O_8P$	363.0580	$[M+H]^+$	364.0653	0	4.84E-14	0.20

Detected m/z	Retention time (min)	Metabolite	Formula	Monoisotopic mass	Adduct	Calculated m/z	Delta (ppm)	Anova (p)	Fold Change (Conrol/ Actinomycin)
382.1013	8.45	Succinyladenosine	$C_{14}H_{17}N_5O_8$	383.1077	$[M-H]^-$	382.1004	2	1.06E-09	0.23
428.0372	8.82	2'-Deoxyguanosine 5'-diphosphate	$C_{10}H_{15}N_5O_{10}P_2$	427.0294	$[M+H]^+$	428.0367	1	1.35E-05	0.22
426.0229	8.90	Adenosine diphosphate	$C_{10}H_{15}N_5O_{10}P_2$	427.0294	$[M-H]^-$	426.0221	2	1.24E-05	0.28
447.0682	9.39	CDP-ethanolamine	$C_{11}H_{20}N_4O_{11}P_2$	446.0604	$[M+H]^+$	447.0677	1	1.29E-05	3.61
489.1152	9.00	Citicoline	$C_{14}H_{27}N_4O_{11}P_2$	489.1152	$[M+H]^+$	489.1152	0	1.35E-04	1.33
533.2514	1.64	PA	$C_{25}H_{43}O_{10}P$	534.2594	$[M-H]^-$	533.2521	1	2.89E-09	0.00
535.2668	1.74	PA	$C_{25}H_{43}O_{10}P$	534.2594	$[M+H]^+$	535.2667	0	5.29E-04	0.01
538.5202	2.19	Cer(d18:1/16:0)	$C_{34}H_{67}NO_3$	537.5121	$[M+H]^+$	538.5194	1	2.65E-04	2.43
538.5202	2.19	Ceramide	$C_{34}H_{67}NO_3$	537.5121	$[M+H]^+$	538.5194	1	7.05E-04	2.15
547.2670	1.64	Antimycin A	$C_{28}H_{40}N_2O_9$	548.2734	$[M-H]^-$	547.2661	2	2.41E-07	0.00
565.0488	9.19	Uridine diphosphate glucose	$C_{15}H_{24}N_2O_{17}P_2$	566.0550	$[M-H]^-$	565.0477	2	1.60E-03	1.09
662.1031	8.47	NAD	$C_{21}H_{27}N_7O_{14}P_2$	663.1091	$[M-H]^-$	662.1018	2	6.63E-07	1.03
752.5584	2.01	PE	$C_{43}H_{78}NO_7P$	751.5516	$[M+H]^+$	752.5589	1	1.07E-06	2.31
779.5209	10.38	PA	$C_{44}H_{75}O_9P$	778.5149	$[M+H]^+$	779.5221	2	1.17E-03	0.11

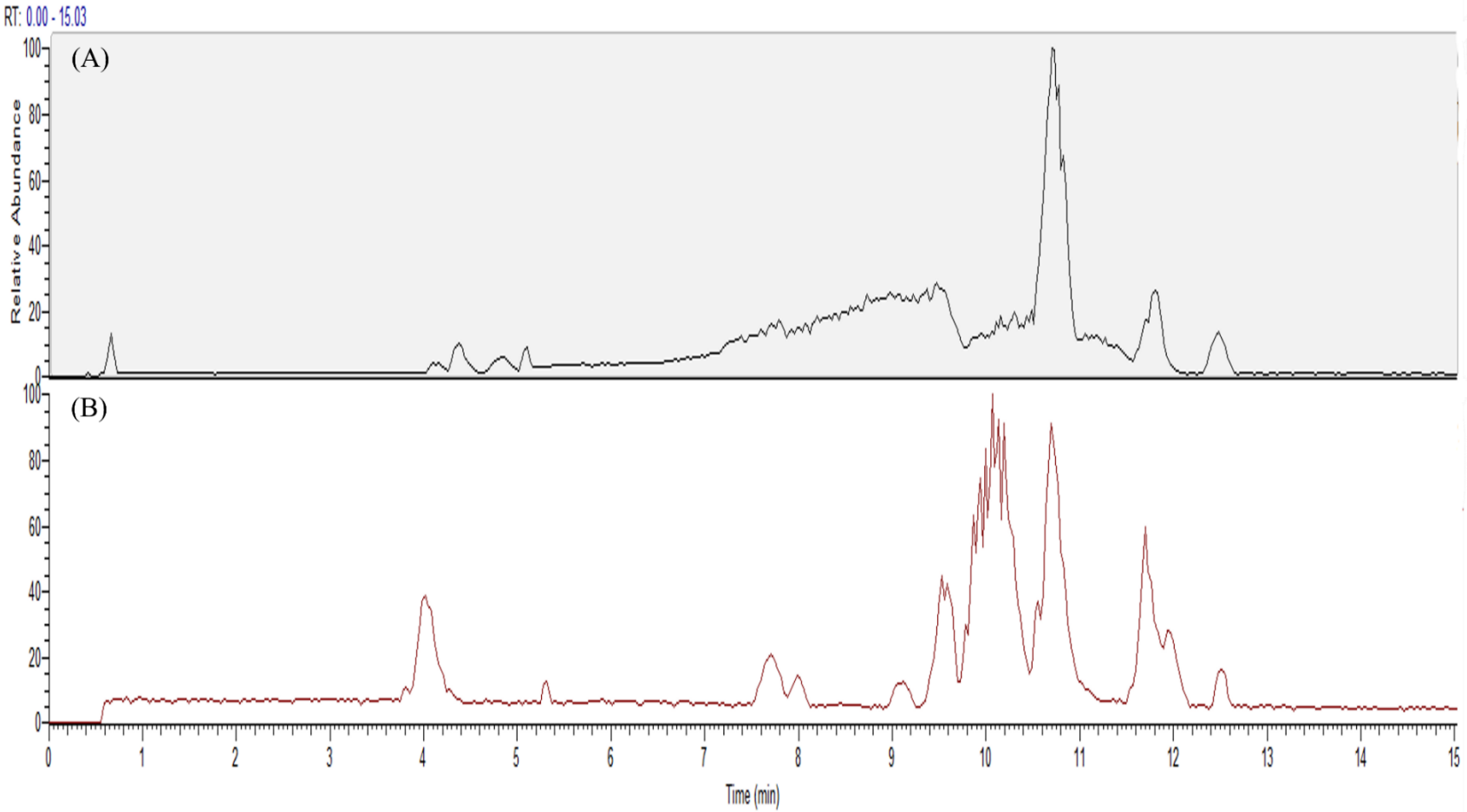

Supplementary Fig.1 Full scan base peak chromatogram of a control (A) and treated cells (B) in ESI-.

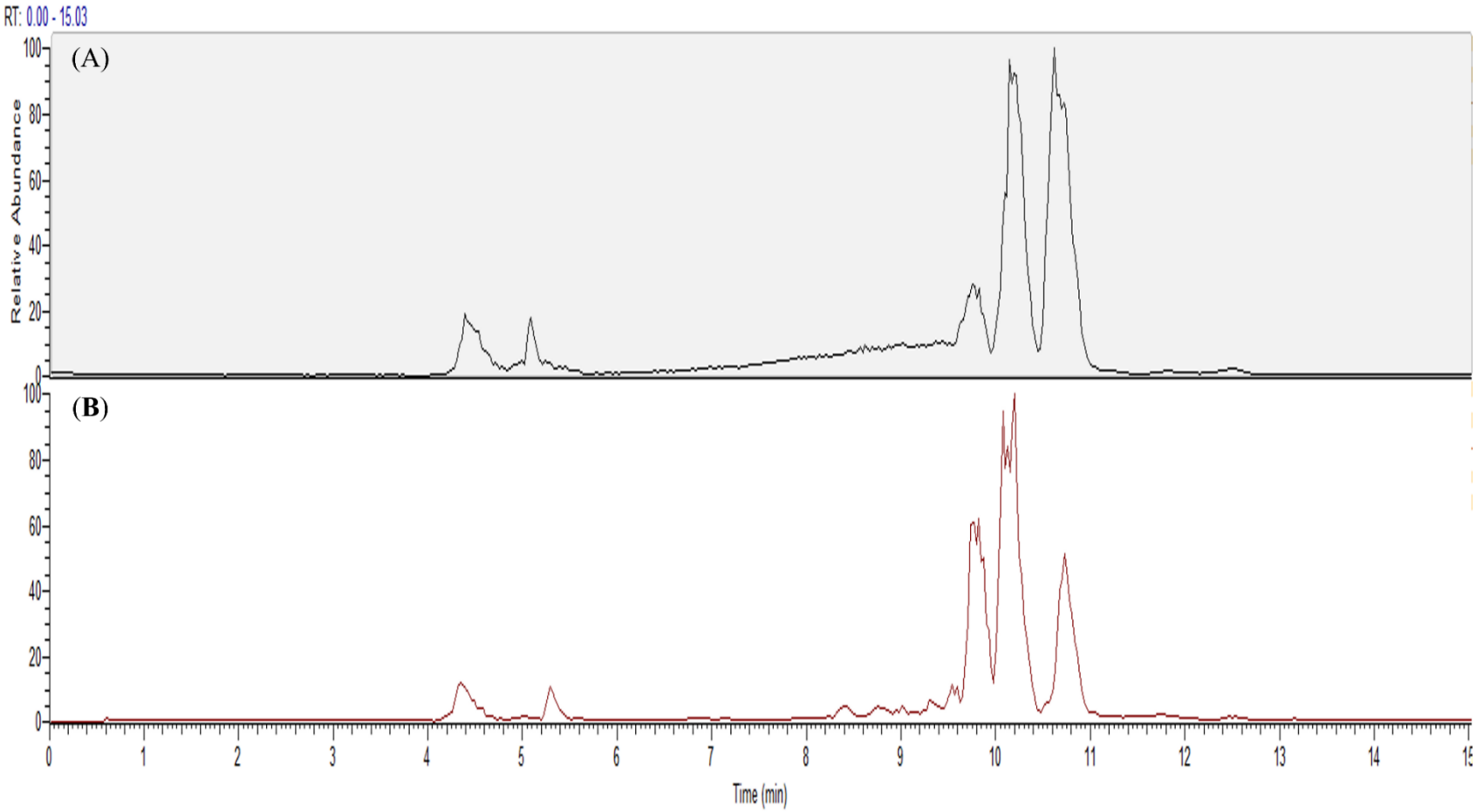

Supplementary Fig.2 Full scan base peak chromatogram of a control (A) and treated cells (B) in ESI+.